J Mater Sci (2015) 50:6437–6443
DOI 10.1007/s10853-015-9198-3

Highly bendable, transparent, and conductive AgNWs-PET films fabricated via transfer-printing and second pressing technique

Mao-xiang Jing[1] · Min Li[1] · Cui-yu Chen[1] · Zhou Wang[1] · Xiang-qian Shen[1]

Received: 5 May 2015 / Accepted: 20 June 2015 / Published online: 30 June 2015

Abstract Highly bendable, transparent, and conductive films composed of silver nanowires (AgNWs) network and polyethylene terephthalate (PET) substrate were prepared by a transfer-printing and second pressing technique using different dimensional AgNWs. The performance of the films as a function of optical and bending performances with low sheet resistance is enhanced, by controlling the diameter and length of AgNWs, area density, and the mechanical press condition. With the optimized mean diameter (D) ~40 nm and length (L) ~15 μm, the as-prepared AgNWs-PET film possesses a sheet resistance of 11.5 Ω/sq, transmittance (T_{550}) of 93.4 %, and haze of 1.23 %. The AgNWs-PET film with the second press treatment at 10 MPa for 20 s shows a very excellent bending performance, with less than 8 % change of the sheet resistance after 46,000 bending cycles without any additional conductive polymer. This highly bendable, transparent, and conductive film is suitable for emerging technologies such as flexible display, electrical skins, and bendable solar cells.

Introduction

Transparent conductive films are essential for the fabrication of touch panels, liquid crystal displays, organic light-emitting diodes (OLEDs), solar cells, and other electronic devices [1–3]. As yet, such transparent films as indium tin oxide (ITO) offer both high transmittance (T ~90 %) and low sheet resistance (R_s < 100 Ω/sq). However, ITO is not a suitable candidate for future high-performance and flexible electronic devices due to its intrinsic brittleness resulting in brittle fracture after 1 % strain [4, 5], and the high processing temperature for deposition that may be unsuitable for flexible polymer materials [6].

Thin films of carbon nanotubes (CNT) [7], graphene nanosheets [8], conductive polymers [9], and metal nanowires [10] have been explored extensively. Among them, CNTs and graphene films were reported with a sheet resistance of 160 Ω/sq at an average transmittance of 87 % [11], and 300 Ω/sq at an average transmittance of 80 % [12], respectively. In comparison, only silver nanowires (AgNWs) films were reported to have a potential to replace ITO [13, 14]. Particularly, AgNWs film shows good bending resistance, which is a major weakness for ITO film. The advantage of flexible properties for AgNWs film promotes it to be widely used in light and portable devices, such as flexible display [15], electrical skins [16], and bendable solar cells [17].

The electrical and optical performances of AgNW films are strongly dependent on the dimension and distribution of individual AgNWs. Takehiro et al. [18] demonstrated the electrodes consisting of AgNWs with a diameter (D) of 70 nm and a length (L) of 8 μm fabricated by the heat treatment process at 150 °C. Khanarian et al. [19] presented their experimental and theoretical results and it was found that to achieve a high transmittance >90 % with a low sheet resistance <100 Ω/sq, and the superfine Ag NWs with D <50 nm and L >5 μm were required.

The bending properties of the films are becoming more and more important for the flexible devices, which greatly depends on the fabrication process. Liu et al. [20] investigated the Meyer rod coating of AgNWs for fabrication of transparent electrodes. The process resulted in a sheet

✉ Xiang-qian Shen
shenxq@ujs.edu.cn

[1] Institute for Advanced Materials, Jiangsu University, Zhenjiang 212013, China

resistance of 175 Ω/sq, optical transparency of 75 %, with a sheet resistance of 2 % change after only 100 bending cycles. Takehiro et al. [18] reported the AgNWs transparent electrodes fabricated by the mechanical press at 25 MPa for 5 s at room temperature. Although the adhesion between the nanowires and substrate was improved, unfortunately, the sheet resistance of the pressed AgNW electrodes increased 19 % after 1000 bending cycles. In order to enhance the electrical conductivity and bending performance, Lee et al. [21] used poly (3,4-ethylenedioxythiophene):poly(styrene sulfonate) (PEDOTE:PSS) as a soldering material to make a highly bendable AgNW/conducting polymer hybrid films with low sheet resistance and high transmittance. The fabricated flexible transparent electrode maintained its conductivity over 20,000 bending cycles, but this process would increase the cost and complexity of the fabrication process due to the additional conductive polymer.

Up to date, AgNWs film could be prepared by a variety of processes, such as vacuum filtration [22], drop-cast method [23], Meyer rod coating [24], air-spraying [25], and transfer-printing technique [26]. However, it is very difficult to achieve a high quality film with low sheet resistance, high optical transmittance, and good adhesion between the nanowires and substrate surface at the same time.

In this work, the AgNWs-polyethylene terephthalate (PET) transparent conductive films with improved conductivity, high transmittance, and good adhesion of AgNWs with substrate were fabricated by the transfer-printing and second pressing technique. The effects of the diameter and length of AgNWs, area density, and the mechanical press condition on the photoelectric properties, interface characteristic, and bending performance were also discussed.

Experimental

Fabrication of AgNWs-PET films

AgNWs with a mean diameter of about 40, 60, and 100 nm, respectively, and a mean length of about 10–15 μm were synthesized by our reported polyol process [27]. First of all, 1 mL AgNWs suspension with a concentration of 10 mg/mL was diluted 1000 times by anhydrous ethanol, and then 1 mL fresh suspension was second diluted 4–10 times to form the final solution with a concentration of 1–2.5 μg/mL. The aim of the dilution process is to control the area density and uniformity of the coated AgNWs film easily by means of the concentration and volume of the suspension. In the dilution process, the ultrasonic dispersion treatment is essential.

Figure 1 shows the schematic illustration of the formation steps for an AgNWs-PET film. Firstly, the AgNWs network was drop-coated onto a polyvinylidene fluoride (PVDF) filter membrane (Φ 45 mm, hole diameter of 0.22 μm) by using the filtration unit of sand core. Then, the PVDF filter membrane with AgNWs was stamped on the PET substrate by using a mechanical tablet machine with a pressure gage and a stop-watch to press them at 0.5–5 MPa for 15 s, tearing the filter membrane slowly, the AgNWs network was transferred onto the PET substrate, and then allowed to dry in air for 3–5 min. Finally, the second press treatment involved mechanically pressing the AgNWs-PET films at 10 MPa for 20 s was aimed to increase the contact between AgNWs and the substrate, and among the nanowires.

Characterization of AgNWs-PET films

Transmittance measurement for AgNWs films was carried out by using an UV–Vis spectrometer (Beijing PGeneral, TU-1900) at the range of 350–900 nm. The sheet resistance of the film in a 20 mm × 20 mm square was measured using the four-probe method, and the values reported in this work were the mean value obtained across the entire film. The structure of the AgNWs on the substrate was observed using a JEOL JSM-7001 scanning electron microscopy (SEM; JEOL Ltd., Tokyo, Japan). The surface roughness of the AgNWs was investigated using a MicroNano D3000 atomic force microscopy (AFM; Shanghai Zhuolun MicroNano Instrument Co., Ltd., China). The bending performance for the fabricated AgNWs-PET films was determined by measuring the sheet resistance change of the films with the bending cycles using a circling machine as schematically shown in Fig. 2, with a film bending radius of 5 mm, and the machine was circled at a speed about 120 cycles/min, the sheet resistance was tested once every 2000 cycles.

Results and discussion

There are generally several parameters that need to be optimized before a uniform coating of nanowires can be achieved. In this study, the AgNWs (mean $D \sim 60$ nm, $L \sim 15$ nm) network is transferred onto the PET substrate by the mechanical press at 0.5–5 MPa for 15 s, and the influence of different pressures imposed on AgNWs-PET films is shown in Fig. 3a. From Fig. 3a, the sheet resistance decreases clearly with the increase of the pressure from 0.5 to 3 Mpa, and the lowest sheet resistance of 29.2 Ω/sq is obtained at the pressure of 3 Mpa. The reason for this phenomenon is that with the increase of the pressure, more and more AgNWs are transferred onto the PET substrate,

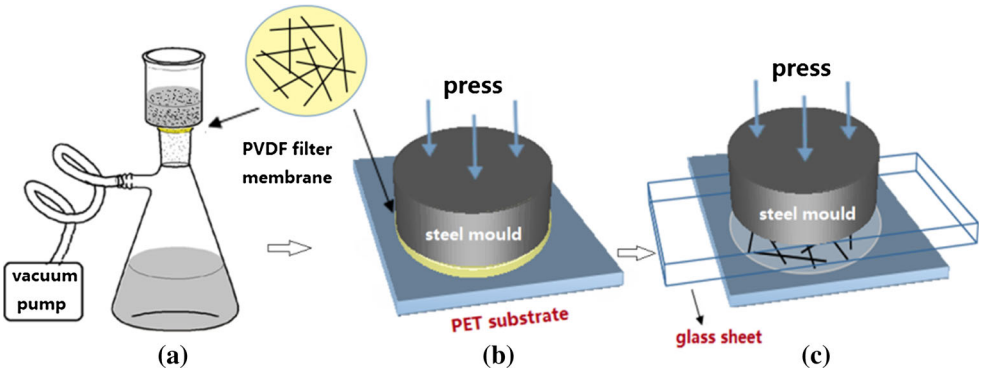

Fig. 1 Schematic illustration of the fabrication of an AgNWs network on PET substrate

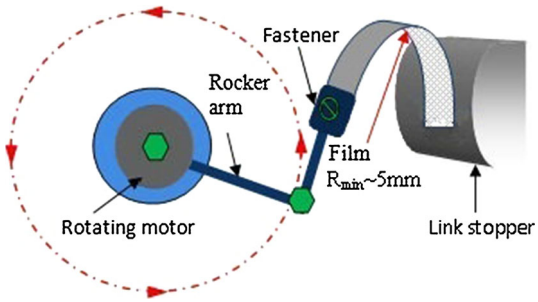

Fig. 2 Schematic illustration of the measurement machine for film bending performance

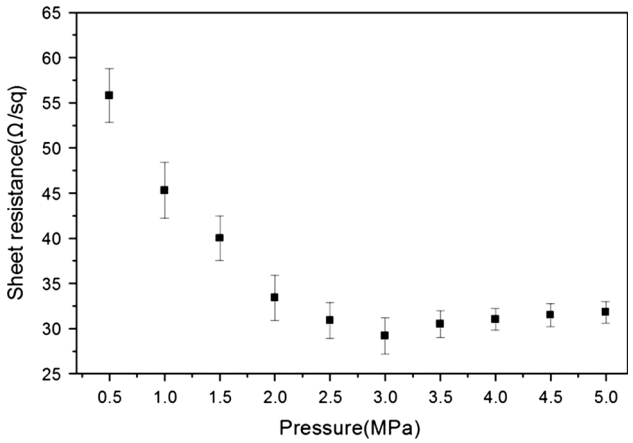

Fig. 3 Change of sheet resistance of AgNWs-PET film with different pressures

and the contact area/point among AgNWs is improved. However, the sheet resistance of AgNWs-PET films rebounds to 32.8 Ω/sq, when the pressure is over 3 Mpa, owing to that too high pressure would prohibit the complete transfer of AgNWs onto the PET substrate as some AgNWs remain still on the surface of the PVDF filter membrane. Therefore, 3 MPa is the optimized pressure in the first transfer-printing step.

To confirm the influence of the diameter and length of AgNWs on the electrical conductivity and optical transmittance of the AgNWs-PET films, the AgNWs with different diameters and lengths were transferred onto PET substrate at 3 MPa for 15 s. Figure 4 presents the SEM morphologies of AgNWs-PET films with different diameters and lengths. It can be seen that the nanowire density on the film increases as the nanowire diameter decreases. The relationship between the transmittance and sheet resistance for AgNWs-PET films with different diameters and lengths is plotted in Fig. 5. It shows that high conductive AgNWs films ($R_s < 60$ Ω/sq) with a good transmittance ($T_{550} > 93$ %) can be obtained using thinner and longer AgNWs. Typically, the films constructed from AgNWs (mean $D \sim 40$, 60 nm, $L \sim 15$ μm) exhibit outstanding performance, which are significantly superior to the films with the diameter of approximately 100 nm and mean length of 10 μm. These thin and long AgNWs enable a high electrical conductivity due to their percolation networks while basically maintaining the optical transparency of the substrate, and better connection networks can be obtained using longer and thinner nanowires, leading a decreased sheet resistance. That is, the sheet resistance at a fixed transmittance decreases as the nanowire diameter decreases and the length increases. For instance, at the transmittance (T_{550}) of 94.3 % or so, the sheet resistance of AgNWs-PET films with mean diameter of 100, 60, and 40 nm of AgNWs is 481, 29.2, and 18.5 Ω/sq, respectively.

At the same suspension concentration, the films constructed from AgNWs (mean $D \sim 40$ nm, $L \sim 15$ μm) have a sheet resistance of 18.5 Ω/sq with an optical transmittance (T_{550}) of 94.3 % while that constructed from AgNWs (mean $D \sim 60$ nm, $L \sim 15$ μm) possesses a sheet resistance of 23.0 Ω/sq with optical transmittance (T_{550}) of 93.6 %, respectively (Fig. 5). Clearly, the sheet resistance decreases for the film with the thinner diameters, which can be attributed to a higher density of junctions in the nanowire networks and an increase of the current paths. In order to achieve a percolation on a random network of AgNWs, the critical density of nanowires can be given by Eq. (1) [28].

$$l\sqrt{\pi N_c} = 4.326, \quad (1)$$

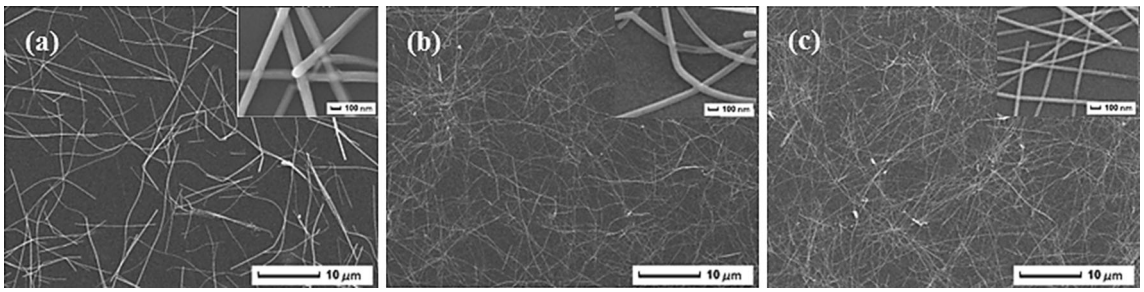

Fig. 4 SEM morphologies of AgNWs-PET films with different diameters and lengths (**a** $D \sim 100 \pm 6$ nm, $L \sim 10 \pm 1.5$ μm; **b** $D \sim 60 \pm 4$ nm, $L \sim 15 \pm 2$ μm; **c** $D \sim 40 \pm 2.7$ nm, $L \sim 15 \pm 1.4$ μm)

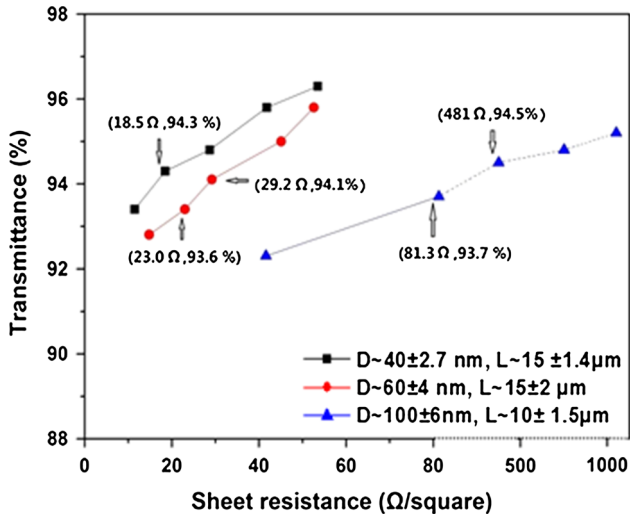

Fig. 5 Transmittance and mean sheet resistance of AgNWs-PET films with different diameters and lengths

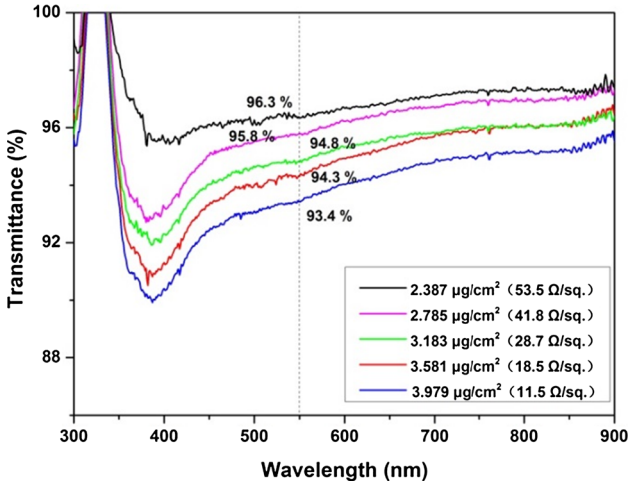

Fig. 6 Transmittance of AgNWs-PET films for various AgNWs area densities with a blank PET as the reference

where l is the length and N_c is the critical density of AgNWs.

It indicates that the critical density to attain the percolation on a random network is not related with the wire diameter but only inversely proportional to the square of the wire length. Meanwhile, according to the percolation model based on randomly distributed nanowires [28], the sheet resistance of a nanowire film has the following relation to the nanowire density (N):

$$R_s \propto (N - N_c)^{-\alpha}, \quad (2)$$

where α is a critical exponent for the conduction, which has a value of 1.33 for 2-D networks and 1.94 for 3-D networks [29, 30]. According to the above formula, with the same wire length, N_c keeps invariant, but when the wire diameter decreases, N would increase, then, the R_s value of the film would be reduced.

The AgNWs diameter also plays an important role for optical properties. It is found in this work the AgNWs film with mean diameter of 40 nm exhibits the highest optical transparency. As the diameter of the AgNWs is smaller than the wavelength of visible light, the light scattering from the metallic silver surface can be reduced significantly in comparison with the larger diameter AgNWs. Subsequently, the film composed of AgNWs with a smaller diameter can achieve better optical properties such as high transmittance and low haze [31].

The sheet resistance and transmittance of the AgNWs-PET films are largely determined by the coating area density of the AgNWs network, which can be adjusted via the concentration and volume of the AgNWs suspension. With the AgNWs (mean $D \sim 40$ nm, $L \sim 15$ μm) suspension solution concentration from 1.5 to 2.5 μg/mL, the area density of the AgNWs network changes from 2.387 to 3.979 μg/cm^2, the transmittance for the films also changes with the different nanowire area densities as shown in Fig. 6. As anticipated, there is a tradeoff between the optical transparency and sheet resistance. It can be observed that the transmittance is higher when the nanowire density is lower, which results in a higher sheet resistance since the number of nanowires is possibly not enough to form the effective conducting network. It is worthwhile to note that with the AgNWs area density of

3.979 μg/cm^2 the sheet resistance is up to 11.5 Ω/sq with the transmittance of 93.4 % at the wavelength of 550 nm (T_{550}). Comparing with the CNT/AgNW films we reported recently [32], these AgNWs-PET films exhibits a better electrical conductivity and higher optical transparency, and they are promising candidates for use in transparent electrodes in tough screens, solar cells, and OLEDs [33, 34].

Figure 7 shows the SEM morphologies of AgNWs-PET films with the AgNWs area density of 2.387, 3.183, and 3.979 μg/cm^2, respectively. The AgNWs are uniformly distributed on the substrate surface to form the nanowire networks.

The bending performance of AgNWs-PET films is important in many applications such as flexible optoelectronic devices. For the bending performance measurement in the present work, the AgNWs-PET film specimens were fabricated from the AgNWs with the mean diameter of 40 nm and mean length of 15 μm, and the AgNWs-PET film was treated with the second press at 10 MPa for 20 s at room temperature.

In general, good bending performance needs high adhesion between AgNWs with PET substrate. Figure 8 shows the change of the sheet resistance for the films with and without second press treatment before and after adhesion measurement by 3 M adhesive tape. It can be seen that the sheet resistance of the film without second press treatment increased from 14.6 to 64.7 Ω/sq with the transmittance change from 93.5 to 96.1 %, while the sheet resistance of the film with second press treatment just increased from 11.5 to 20.3 Ω/sq with a little change of transmittance. The result illustrates that the adhesion performance of the AgNWs film was greatly improved by second pressing.

The sheet resistance change of the AgNWs-PET films as a function of bending cycles is shown in Fig. 9. Thereinto, the R/R_0 means the ratio of the sheet resistance after bending cycles to the original values before bending cycles. It can be seen that for the film without the second press treatment, the sheet resistance begins to rise after only 6000 bending cycles, and then increases more than 50 % after 40,000 cycles. The bending cycles for the film without the second press treatment is limited owing to the low adhesion between AgNWs with PET substrate, and the AgNWs junctions could be detached and the nanowires slide against each other to cause a high contact resistance. It is interesting for the AgNWs-PET films with the second press treatment. The sheet resistance has a very low change less than 8 % even after 46,000 bending cycles due to the

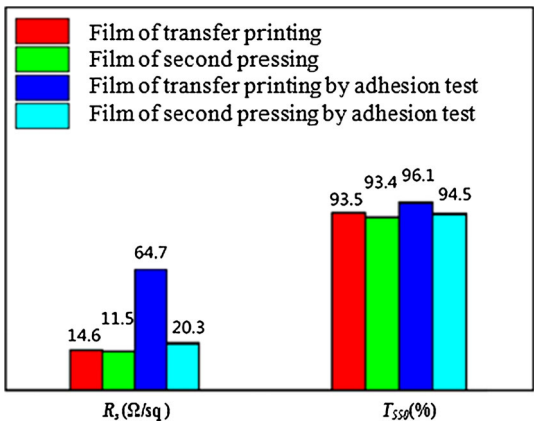

Fig. 8 Adhesion test of the films with and without second press treatment

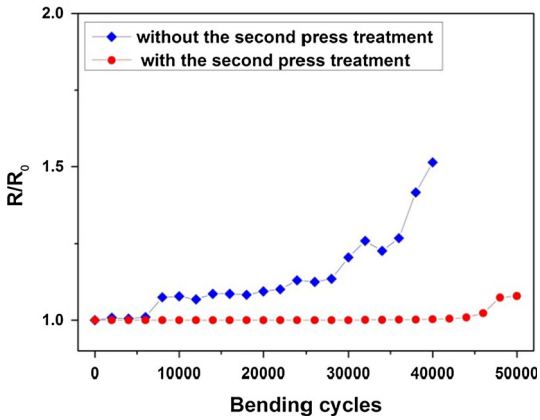

Fig. 9 The mean sheet resistance ratios of AgNWs-PET films with and without the second press treatment as a function of bending cycles

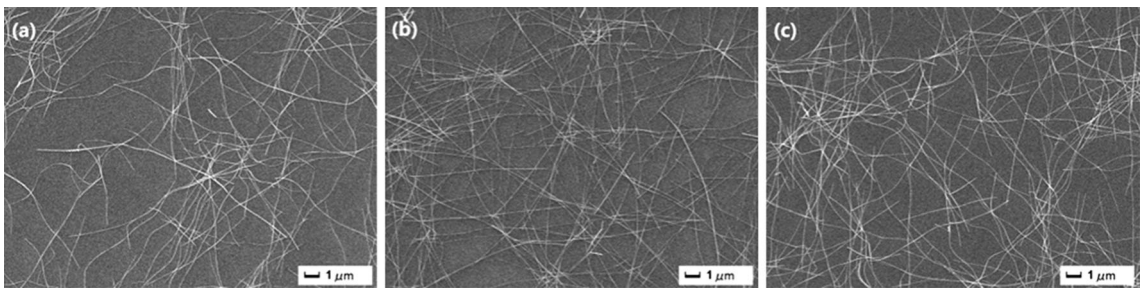

Fig. 7 SEM morphologies of AgNWs-PET films with different area densities. **a** 2.387 μg/cm^2, **b** 3.183 μg/cm^2, and **c** 3.979 μg/cm^2

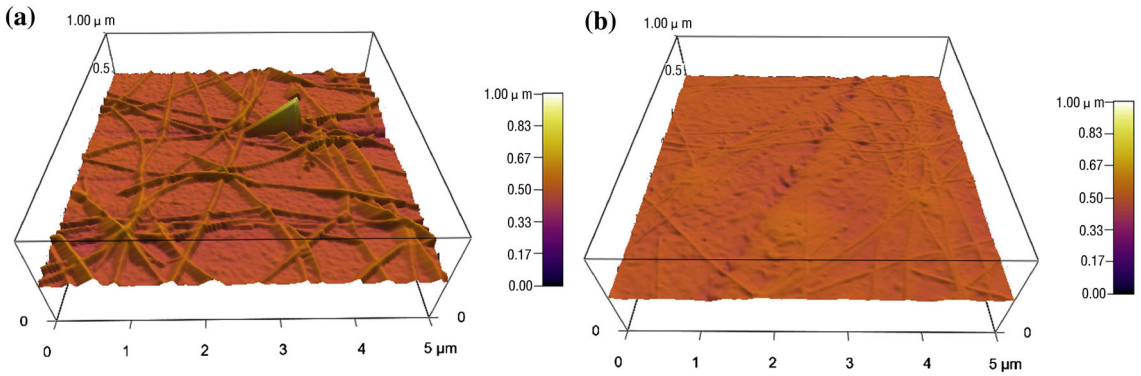

Fig. 10 AFM images of AgNWs-PET film. **a** Without second press treatment. **b** With second press treatment

tight junctions between AgNWs and with substrate. Up to date, in comparison with the bending performance of the AgNWs-PET films reported by other researchers [18, 21], the prepared AgNWs-PET film with the second press treatment in this work possesses less sheet resistance increase with longer bending cycles.

The surface structures of the films with and without the second press treatment were studied by AFM as shown in Fig. 10. It can be observed from Fig. 10 that the surface roughness of the AgNWs-PET films with and without the second press treatment is greatly different. The AgNWs for the film without the second press treatment are generally floating on the PET surface. While with the second press treatment (Fig. 10b), the film surface becomes much smoother and the nanowires seem to be embedded in the near surface of the PET substrate. The surface roughness decreases from about 31 nm (Fig. 10a) to 10 nm (Fig. 10b), and the haze of the film also decreases from 6.7 to 1.23 % which is extremely significant for the use of AgNWs-PET films in touch panels and OLEDs [35]. Combining Figs. 8, 9, and 10, the surface roughness could influence the optical and electrical properties and the bending performance. Low roughness could result in low sheet resistance and good bending performance, but little influence on transmittance. The improved conductivity and bending performance is possibly due to the diffusion and deformation of AgNWs during the pressing process, leading to a low surface roughness and a strong physical bonding between the AgNWs and with the PET substrate.

Conclusions

(1) The highly bendable, transparent, and conductive AgNWs-PET films were fabricated via the transfer-printing and second pressing technique.

(2) The electrical conductivity and optical transmittance of the films are largely influenced by the AgNWs networks formed on the PET substrate surface, which can be controlled by the diameter and length of AgNWs, coating area density, and mechanical press conditions. With the optimized AgNWs (mean $D \sim 40$ nm, $L \sim 15$ μm), the film exhibits the best electrical and optical properties, with $T_{550} \sim 93.4$ %, $R_s \sim 11.5$ Ω/sq, and haze of 1.23 %.

(3) It is found that the bending performance for the AgNWs-PET films is closely related to the adhesion between AgNWs and the PET substrate, which is strongly influenced by the mechanical press process. For the AgNWs-PET films fabricated from AgNWs with mean $D \sim 40$ nm, $L \sim 15$ μm and treated with the second press at 10 MPa for 20 s, the sheet resistance change is less than 8 % after 46,000 bending cycles, and this kind of AgNWs-PET films is suitable for forthcoming technologies such as flexible display, electrical skins, and bendable solar cells.

Acknowledgements This work was financially supported by the National Natural Science Foundation of China (Grant Nos. 51274106, 51474113, 51474037), the Science and Technology Support Program of Jiangsu Province of China (Grant Nos. BE2012143, BE2013071, BE2014850), the Natural Science Research Program of Jiangsu Province Higher Education of China (Grant Nos. 12KJA430001, 14KJB430010), and the Jiangsu Province's Postgraduate Cultivation and Innovation Project of China (Grant CXZZ13-0662, KYLX-1030, SJZZ-0132).

Compliance with Ethical Standards

Conflict of interest The authors declare that they have no conflict of interest.

References

1. Ham J, Lee JL (2014) ITO breakers: highly transparent conducting polymer/metal/dielectric (P/M/D) films for organic solar cells. Adv Energy Mater 4:11–15

2. Yim JH, Joe S, Pang C, Lee KM, Jeong H, Park JY, Yeong AH, Mello JC, Lee S (2014) Fully solution-processed semitransparent organic solar cells with a silver nanowire cathode and a conducting polymer anode. ACS Nano 8(3):2857–2863
3. Ham J, Kim S, Jung GH, Dong WJ, Lee JL (2013) Design of broad band transparent electrodes for flexible organic solar cells. J Mater Chem A 1:3076–3082
4. Liu BT, Kuo HL (2013) Graphene/silver nanowire sandwich structures for transparent conductive films. Carbon 63:390–396
5. Liu BT, Hsu CH (2011) Anti-scratch and transparency properties of transparent conductive carbon nanotube films improved by incorporating polyethoxysiloxane. J Colloid Interface Sci 359(2):423–427
6. Tien WC, Chu AK (2014) ITO DBR electrodes fabricated on PET substrate for organic electronics. Opt Express 22:3944–3949
7. Liu BT, Hsu CH, Wang WH (2012) A comparative study on preparation of conductive and transparent carbon nanotube thin films. J Taiwan Inst Chem Eng 43(1):147–152
8. Tien HW, Huang YL, Yang SY, Hsiao ST, Wang JY, Ma CCM (2011) Graphene nanosheets deposited on polyurethane films by self-assembly for preparing transparent, conductive films. J Mater Chem 21(38):14876–14883
9. Yang L, Kong J, Yee WA, Liu W, Phua SL, Toh CL et al (2012) Highly conductive graphene by low-temperature thermal reduction and in situ preparation of conductive polymer nanocomposites. Nanoscale 4(16):4968–4971
10. Singh V, Joung D, Zhai L, Das S, Khondaker SI, Seal S (2011) Graphene based materials: past, present and future. Prog Mater Sci 56(8):1178–1271
11. Zhang DH, Ryu K, Liu XL, Polikarpov E, Ly J, Tompson ME, Zhou CW (2006) Transparent, conductive, and flexible carbon nanotube films and their application in organic light-emitting diodes. Nano Lett 6(9):1880–1886
12. Tung VC, Allen MJ, Yang Y, Kaner RB (2009) High throughput solution processing of large-scale graphene. Nat Nanotechnol 4:25–29
13. Amjadi M, Pichitpajongkit A, Lee S, Ryu S, Park I (2014) Highly stretchable and sensitive strain sensor based on silver nanowire-elastomer nanocomposite. ACS Nano 8:5154–5163
14. Coskun S, Ates ES, Unalan HE (2013) Optimization of silver nanowire networks for polymer light emitting diode electrodes. Nanotechnology 24:125202
15. Lee J, Lee P, Lee H, Lee D, Lee SS, Ko SH (2012) Very long Ag nanowire synthesis and its application for a highly transparent, conductive and flexible metal electrode touch panel. Nanoscale 4:6408–6414
16. Takei K, Takahashi T, Ho JC, Ko H, Gillies AG, Leu PW, Fearing RS, Javey A (2010) Nanowire active-matrix circuitry for low-voltage macroscale artificial skin. Nat Mater 9:821–826
17. Lipomi DJ, Tee BCK, Vosgueritchian M, Bao Z (2011) Stretchable organic solar cells. Adv Mater 23:1771–1775
18. Takehiro T, Masaya N, Makoto K, Jinting J, Thi TN, Yoshio A, Katsuaki S (2011) Fabrication of silver nanowire transparent electrodes at room temperature. Nano Res 4(12):1215–1222
19. Khanarian G, Joo J, Liu XQ, Eastman P, Werner D, Connell KO, Trefonas P (2013) The optical and electrical properties of silver nanowire mesh films. J Appl Phys 114:024302
20. Liu CH, Yu X (2011) Silver nanowire-based transparent, flexible, and conductive thin film. Nanoscale Res Lett 6:75
21. Lee J, Lee P, Lee HB, Hong SK, Lee I, Yeo J, Lee SS, Kim TS, Lee DJ, Ko SH (2013) Room-temperature nanosoldering of a very long metal nanowire network by conducting-polymer-assisted joining for a flexible touch panel application. Adv Funct Mater 23:4171–4176
22. De S, Higgins TM, Lyons PE, Doherty EM, Nirmalraj PN, BlauWJ BJ, Coleman JN (2009) Silver nanowire networks as flexible, transparent, conducting films: extremely high DC to optical conductivity ratios. ACS Nano 3(7):1767–1774
23. Yu ZB, Zhang QW, Li L, Chen Q, Niu XF, Liu J, Pei Q (2011) Highly flexible silver nanowire electrodes for shape-memory polymer light-emitting diodes. Adv Mater 23(5):664–668
24. Li X, Gittleson F, Carmo M, Sekol RC, Taylor AD (2012) Scalable fabrication of multifunctional freestanding carbon nanotube/polymer composite thin films for energy conversion. ACS Nano 6(2):1347–1356
25. Kim T, Canlier A, Kim GH, Choi J, Park M, Han SM (2013) Electrostatic spray deposition of highly transparent silver nanowire electrode on flexible substrate. ACS Appl Mater Interfaces 5:788–794
26. Gaynor W, Burkhard GF, McGehee MD, Peumans P (2011) Smooth nanowire/polymer composite transparent electrodes. Adv Mater 23(26):2905–2910
27. Li M, Jing MX, Wang Z, Li B, Shen XQ (2015) Controllable growth of superfine silver nanowires by self-seeding polyol process. J Nanosci Nanotechnol 15:6088–6093
28. Kiran Kumar ABV, Bae CW, Piao LH, Kim SH (2013) Silver nanowire based flexible electrodes with improved properties: high conductivity, transparency, adhesion and low haze. Mater Res Bull 48:2944–2949
29. Lee HS, Kim YW, Kim JE, Yoon SW, Kim TY, Noh JS, Suh SK (2015) Synthesis of dimension-controlled silver nanowires for highly conductive and transparent nanowire films. Acta Mater 83:84–90
30. Madaria AR, Kumar A, Ishikawa FN, Zhou CW (2010) Uniform, highly conductive, and patterned transparent films of a percolating silver nanowires network on rigid and flexible substrates using a dry transfer technique. Nano Res 3:564–573
31. De S, Higgins TM, Lyons PE, Doherty EM, Nirmalraj PN, Blau WJ, Boland JJ, Coleman JN (2009) Silver nanowire networks as flexible, transparent, conducting films: extremely high DC to optical conductivity ratios. ACS Nano 3:1767–1774
32. Jing MX, Han C, Li M, Shen XQ (2014) High performance of carbon nanotubes/silver nanowires-PET hybrid flexible transparent conductive films via facile pressing-transfer technique. Nanoscale Res Lett 9:588
33. Yu Z, Zhang Q, Li L, Chen Q, Niu X, Liu J, Pei Q (2011) Highly flexible silver nanowire electrodes for shape-memory polymer light-emitting diodes. Adv Mater 23:664–668
34. Zhang YY, Wang LC, Li X, Yi XY, Zhang N, Li J, Zhu HW, Wang GH (2012) Annealed InGaN green light-emitting diodes with graphene transparent conductive electrodes. J Appl Phys 111:114501
35. Hwang JO, Park JS, Choi DS, Kim JY, Lee SH, Lee KE, Kim YH, Song MH, Yoo S, Kim SO (2012) Work function-tunable, N-doped reduced graphene transparent electrodes for high-performance polymer light-emitting diodes. ACS Nano 6:159–167